Controlling shape morphing and cell release in engineered living materials

Laura K. Rivera-Tarazona[a+], Manivannan Sivaperuman Kalairaj[a+], Tyler Corazao[b], Mahjabeen Javed[a], Philippe E. Zimmern[c], Sargurunathan Subashchandrabose[d], Taylor H. Ware[a,b,*]

[a] Department of Biomedical Engineering, Texas A&M University, College Station, TX, 77843, USA

[b] Department of Materials Science and Engineering, Texas A&M University, College Station, TX, 77843, USA

[c] Department of Urology, The University of Texas Southwestern Medical Center, Dallas, TX, 75390, USA

[d] Department of Veterinary Pathobiology, Texas A&M University, College Station, TX, 77843, USA

* Corresponding author: E-mail: taylor.ware@tamu.edu

+ Authors contributed equally.

Abstract

Engineered living materials (ELMs) derive functionality from both a polymer matrix and the behavior of living cells within the material. The long-term goal of this work is to enable a system of ELM-based medical devices with both mechanical and bioactive functionality. Here, we fabricate multifunctional, stimuli-responsive ELMs comprised of acrylic hydrogel matrix and *Escherichia coli*. These ELMs undergo controlled changes in form and have a controlled release of bacteria from the composite. We hypothesize that the mechanical forces associated with cell proliferation within a covalently-crosslinked, non-degradable hydrogel are responsible for both phenomena. At constant cell loading, increased hydrogel elastic modulus significantly reduces both cell delivery and volume change associated with cell proliferation. ELMs that change

volume over 100% also result in ~10^6 colony forming units / mL in the growth medium over two hours after 1 day of growth. At constant monomer feed ratios, increased cell loading leads to significantly increased cell delivery. Finally, these prokaryotic ELMs were investigated for their potential to deliver a probiotic that can reduce the proliferation of a uropathogen *in vitro*. Controlling the long-term delivery of bacteria could potentially be used in biomedical applications to modulate microbial communities within the human body.

Keywords: Engineered living materials, bacteria, cell delivery, shape change, hydrogels

1. Introduction

Engineered living materials (ELMs) are a class of materials that use living organisms incorporated into biomaterial matrices. These composites derive their multifunctionality from both the living cells, which are principally bacteria or yeast, and non-living components. The biological activity of living cells, which optionally can be genetically engineered, enables a wide variety of metabolism-powered functionalities [1–5]. The non-living component of ELMs is frequently a hydrogel that maintains the survival of the living microorganisms by facilitating the diffusion of water, nutrients, gases, and biomolecules and mechanically contains the microorganism [4]. Natural and synthetic hydrogels have been widely used to synthesize ELMs [6–8].

ELMs can be engineered to best suit desired functionalities for diverse applications [1–5][9,10]. For example, ELMs can serve as components of biosensing, therapeutic, self-healing, and shape-morphing devices [9–12]. ELMs have been designed to elute growth factors to direct stem cell differentiation [13]. Bacterial matrices have been fabricated with adhesive properties for potential treatment of chronic inflammation [14]. Encapsulated bacteria in 3D printed constructs have been fabricated to secrete antibiotics and inhibit the growth of gram-negative

bacteria [15]. In each of these cases, the biochemical activity of the living organism enables a potential biomedical application.

In addition to biochemically-active ELMs, the activity of living cells within ELMs can function to create materials with dynamic mechanical properties. Biomineralization can be used to heal damage in concrete [16]. Contraction of muscle cells can be used to drive locomotion in soft, living robots [17]. We have previously reported that yeast proliferation within polyacrylamide hydrogels can be controlled to drive complex shape transformations in materials. [18]. The *Saccharomyces cerevisiae* cell wall has a Young's modulus of approximately 110 MPa [19], which is much greater than that the Young's modulus of the synthesized soft matrices (10's kPa). We have shown that the proliferation of these relatively stiff cells, causes ELM volumetric expansions. Using this phenomenon, ELMs with yeast probiotics were designed to create drug reservoirs that ruptured and delivered a model drug in response to a biochemical cue [20]. Nevertheless, the use of yeast for delivery and therapeutic applications within the body is limited as there is only a recognized single probiotic yeast strain, *Saccharomyces boulardii* [21]. For the purpose of using ELMs as future delivery platforms in the human body, probiotic bacteria may provide more versatility [22,23]. For example, *E. coli* also has a stiff cell envelope with Young's modulus between 50-150 MPa and exists in probiotic forms [24]. Basic questions remain regarding the feasibility of creating shape changing, bacteria-based ELMs based on cellular proliferation [4][6–8].

The properties of the matrix that contains the living cells in the ELM partially modulate interactions of the cells with the surrounding environment [25,26]. For example, the properties of the hydrogel can control the escape of the embedded cells from the ELM. Frequently, the engineering of a matrix capable of preventing cell escape is necessary to avoid the unwanted

release of genetically modified cells. For example, a tough hydrogel material was designed as a biocontainment platform to prevent the escape of genetically engineered bacteria capable of sensing and responding to specific biomolecules [27]. In another example, *Staphylococcus epidermis* encapsulated within a membrane-in-gel patch was fabricated to secrete beneficial factors that act against skin pathogens [28]. Many other ELMs do not fully retain cells within the encapsulating matrix, and cells that escape can proliferate within the surrounding media [20,21,29–32].

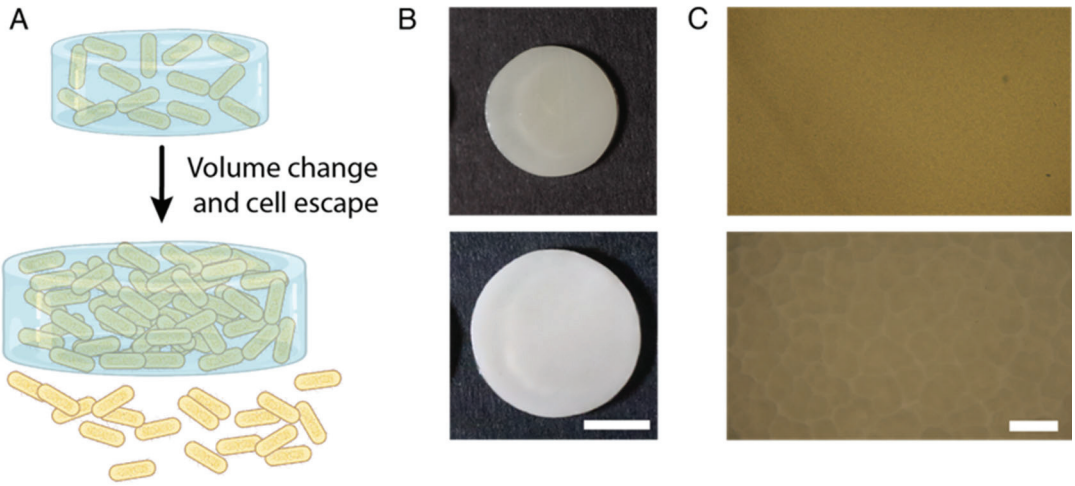

Figure 1: Prokaryotic ELM volume change
(A) Schematic of an ELM encapsulating *E. coli*. The ELM is capable of changing in volume and delivering cells to the surroundings due to cellular proliferation. (B) ELMs change in volume over time as seen before incubation (Top) and after incubation for 72 h (Bottom) (Scale bar: 5 mm). (C) Reflection micrograph of ELM before incubation (Top) and after incubation for 72 h (Bottom) (Scale bar: 200 μm).

Here, we introduce a method to control, at least partially, the delivery of bacteria from ELM hydrogels with different stiffnesses and cell loadings. This cell delivery occurs within ELMs that are simultaneously undergoing shape change, which will potentially enable multifunctional medical devices. The bacterial strain, ampicillin-resistant *E. coli* DH5α, embedded within non-degradable, crosslinked poly(2-hydroxyethyl acrylate) matrices, form ELMs that change shape due to cell proliferation (Fig. 1a). Due to the forces that drive these

shape changes, the cells found on or near the surface of the ELMs can be delivered from the ELM hydrogel and freely proliferate in the surrounding growth media (Fig. 1a). We perform a series of experiments to quantify and control cell delivery by modulating the stiffness and initial cell loading in ELMs. Finally, with controlled cell delivery from ELMs, we demonstrate a potential therapeutic material by releasing a probiotic *E. coli*, asymptomatic bacteriuria (ABU 83972), which then modulates the proliferation of a uropathogenic *E. coli* (UPEC) strain, CFT073, *in vitro*.

2. Materials and methods

2.1 Materials

2-Hydroxyethylacrylate (HEA), *N*,*N*′-methylenebisacrylamide (BIS), ammonium persulfate (APS), kanamycin sulfate, sodium chloride, and agar were purchased from Sigma-Aldrich. Yeast extract, tryptone, ampicillin sodium salt, *N*,*N*,*N*′,*N*′-tetramethylethylenediamine (TEMED), and PBS tablets were purchased from Fisher Scientific. All chemicals were used as received without further purification.

2.2 Bacterial growth and quantification for encapsulation in ELMs

To grow bacteria to a high density, *E.coli* DH5α (transformed with pAAV-Syn-GFP plasmid) were first incubated for 7 h in culture tubes containing 7 mL of Lysogeny Broth (LB-amp) media [0.5 wt % yeast extract, 1 wt % tryptone, 1 wt % sodium chloride, and 50 μg of ampicillin per mL of media] at 37 ºC in a shaking incubator at 200 RPM. Subsequently, bacteria overgrowths were cultured for 14 h in twelve flasks, each containing cultures from 2 overnight tubes and 50 mL of LB-amp media, at 37 ºC and 200 RPM. Overgrowths were combined, and cell density was measured to calculate the volume needed to reach approximately 5.7×10^{11} cells, as measured with the UV-vis, to obtain a high cell density. Cells were centrifuged, washed

three times in PBS, and then centrifuged to obtain a pellet. For ELMs with medium and low cell densities, pellets with 5.7×10^{10} cells and 5.7×10^{9} cells were collected.

To quantify cell density, a Genesys 10S UV/visible spectrophotometer was used to observe the optical density at 600 nm of cell suspensions. Each of the pellets collected was suspended in 25 mL of PBS. Then, 0.1 mL of the initial suspension was mixed with 0.9 mL of PBS, and ten-fold serial dilutions from 1:10 to 1:1000 were made (n = 3). Diluted bacterial solutions were pipetted into a 1-mL cuvette for spectrophotometer measurements. Optical densities between 1.6 and 0.03 were measured for these dilutions.

2.3 Mold construction

For volume change and cell release experiments, molds were used to create flat sheets of the ELMs. Molds were made of two glass slides (75 mm by 51 mm) sterilized with heat and then allowed to cool. The unpolymerized material was sandwiched between the glass slides, separated by a 0.25 mm thick spacer. For mechanical testing, the unpolymerized material was sandwiched between the glass slides, separated by a 1-mm thick spacer. For ABU-containing ELMs, the unpolymerized material was sandwiched between the glass slides, separated by a 0.5-mm thick spacer.To fabricate ELMs that do not need to be cut after polymerization, a 0.25 mm thick polystyrene spacer (75 mm × 51 mm) was cut with a biopsy punch of 10 mm diameter. The unpolymerized material was then filled in the hole, sandwiched between two glass slides (75 mm × 51 mm), and polymerized.

2.4 Preparation of prokaryotic ELMs

Prokaryotic ELMs were prepared at room temperature by free radical polymerization of HEA monomer and BIS crosslinker. HEA was filter sterilized prior to ELM preparation. Stock solutions of BIS (0.02 g/ml) were prepared in dH_2O and filter sterilized. All ELMs with varying

crosslinking densities were prepared with high cell densities and using either 10 wt % HEA with 0.1 wt% BIS and 15 wt% HEA with 0.4 wt% BIS. The concentration of each component denotes the wt% in the entire pre-gel solution, including cells. ELMs with varying cell densities were prepared using 10 wt% HEA and 0.1 wt% BIS with cell loadings of 3×10^{10} cells/mL and 3×10^{9} cells/mL. In these formulations, as biomass decreases media content increases. To polymerize ELMs with varying crosslinker density, a 10 wt% APS stock solution was added at 1% of the total solution volume, and TEMED was added at a ratio of 0.1% of total solution volume. To polymerize ELMs with medium cell loading, the APS solution was added at 1.3% of the total solution volume, and TEMED was added at a ratio of 0.13% of total solution volume. To polymerize ELMs with low cell loading, APS was added at 1.5% of the total solution volume, and TEMED was added at a ratio of 0.15% of total solution volume. After adding APS and TEMED to all pre-gel solutions, the solutions were vortexed for 3 s and quickly pipetted into the molds. Filled molds were flipped every 45 s while polymerization occurred to avoid settling of the bacteria. After 10 min, polymerized ELMs were de-molded and rinsed three times with LB-amp media to remove unpolymerized monomer residues. ELMs were stored in LB-amp at 4 ºC for 24 h to enable the ELM to swell to equilibrium while limiting cell proliferation before mechanical testing, volume change, and cell release experiments.

2.5 Volume change quantification

To quantify volume changes in prokaryotic ELMs, samples were molded in 0.25-mm thick molds. All ELMs were stored in LB-amp for 24 h at 4 ˚C prior to growth test. All ELMs were cut with a biopsy punch of 10 mm diameter to make ELM disks (n = 3 for each type of formulation). The dimensions of each disk were measured immediately before transfer to the flask for growth. All ELM formulations (n = 3) were grown in 250 mL flasks with 150 mL of

LB-amp (3 gels per flask) for 72 h at 37 ºC in aerobic conditions with constant agitation (200 RPM). Volume changes were measured every 24 h using a Canon Rebel T7i camera.

2.6 Cell release quantification

All ELM formulations were molded and stored as described in the volume change quantification section. After storage at 4 ˚C, ELMs were punched (n = 3) and washed three times in PBS. Each sample was placed in 50 mL of LB-amp media. All values presented regarding cell release represent the number of cells per mL of media. Before incubation, an aliquot (100 μL) of media for all formulations was plated on LB-amp agar plates (1.5 wt% agar) using sterile glass beads that were shaken back and forth on the plate for around one minute. All samples were incubated at 37 ºC under constant shaking (200 RPM) and aerobic conditions. After 30 min and 2 h, an aliquot (100 μL) of growth media was diluted (10-fold dilutions) and plated on LB-amp agar plates using glass beads plating technique. The same procedure was followed after ELM formulations were incubated for 24 h, 48 h, or 72 h. Plates were incubated at 37 ºC and colony forming units (CFU) were counted after one day of incubation. We note that this method quantifies both released cells and cells that result from the proliferation of released cells. To better quantify the number of released cells as compared to cells that proliferated in the media, we measured the number of CFU in growth media under two conditions. In condition 1, the ELM is placed in fresh media for 30 mins and then removed. CFUs were counted immediately and again 90 mins later. In condition two, the ELM remained in the media for the entire two hours, and CFUs were counted at both 30 mins and 2 hours. Each day the ELMs were washed and placed into fresh LB media at 37 ˚C shaken at 200 RPM. The release was measured again under conditions 1 and 2 for two days.

2.7 Cell viability quantification

To quantify the number of colony forming units after exposure to each monomer solution and at each nominal cell loading, all ELM formulations were prepared as described in section 2.4 except that APS and TEMED were omitted to prevent gelation. Control solutions were prepared by replacing all monomers with LB-amp. An additional formulation (20HEA/0.4BIS) with high cell loading was also prepared. All controls and monomer solutions were prepared and then the cells were added. After 2 min and 10 min, an aliquot (100 μL) of the formulation was diluted (10-fold dilutions) and plated on LB-amp agar plates using glass beads plating technique. Plates were incubated at 37 ºC, and colony forming units (CFU) were counted after one day of incubation.

2.8 Mechanical characterization

All ELM samples for mechanical testing were cut into disks (6 mm diameter, 1 mm thickness). Samples were equilibrated in LB-amp media for 24 h at 4 ˚C prior to testing. Compression testing was performed using a TA RSA-G2 instrument at room temperature. Briefly, flat plates attached to the instrument were brought into contact with the sample, and a bath attachment was placed to run the testing under immersion in LB-amp media at room temperature. The plates were then set to move at a rate of 0.05 mm/s. Strains between 0.2 % and 5% were used to calculate the Young's modulus, as the stress-strain response in this region was linear.

2.9 Optical images of living composites

Optical imaging was carried out using a Nikon optical microscope. To visualize embedded bacteria and cell proliferation, samples were observed under bright field and dark field

at 10X magnification. Bright field (transmission) was used to observe cell distribution and colony formation. Dark field (reflection) was used to visualize the surface of the samples (n = 3).

2.10 Competition experiments

To perform competition experiments, a probiotic strain of *E. coli*, that causes asymptomatic bacteriuria (ABU 83972) and an uropathogenic (UPEC) *E. coli* strain, CFT073 A1 Tn7 tag KanR, were utilized in this study. Briefly, ELMs (10HEA/0.1BIS) with high concentration of ABU 83972 were synthesized and refrigerated (4º C) overnight in LB media. Separately, UPEC strain was inoculated in 25 mL of LB-Kan media [0.5 wt % yeast extract, 1 wt % tryptone, 1 wt % sodium chloride, and 50 μg of Kanamycin per mL of media] and grown overnight at 37 ºC at 200 RPM. The next day, ABU ELMs were cut into 10 mm diameter disks with a thickness of 0.5 mm. One ABU ELM was placed in 50 mL of LB media in a 250 mL flask and UPEC was inoculated from the overnight culture at a 1:1 ratio (encapsulated ABU:free-floating CFT) (n = 3). ABU ELMs and UPEC were incubated for a total of 24 h. At 0 h, 4 h, 8 h, and 24 h of incubation, an aliquot (100 μL) of the incubation media were plated in LB-Kan agar plates (1.5 wt% agar) using bead plating technique. At each timepoint, the aliquots were diluted appropriately to allow CFU counting after petri dishes were incubated at 37 ºC. *E. coli* strain CFT073 A1 Tn7 tag KanR is Kan resistant, and ABU 83972 is Kan sensitive. As such, only the CFT073 is able to form colonies in the LB-Kan-agar plates. Hence, the CFU measured from the LB-Kan agar plates represent the number of viable UPEC cells present in the co-culture. Separately, free-floating UPEC were incubated with control hydrogels (no ABU) of the same formulation (n = 3) under the same conditions. At 0 h, 4 h, 8 h, and 24 h of incubation, aliquots of the incubation media were plated in LB-Kan-agar plates. Only the colonies of UPEC were counted. The experimental and control samples were compared for competition analysis.

2.11 Statistical analysis

Statistical comparisons were studied using Student's *t*-test (paired or unpaired) or one-way ANOVA (followed by a post-hoc Tukey test) (GraphPad Prism 9). Data are shown as the mean $\pm$ standard deviation. For all studies, a $P < 0.05$ was utilized to consider the results significantly different.

3. Results and discussion

3.1 Fabrication and characterization of prokaryotic ELMs

A series of ELMs with *E. coli* embedded within acrylic hydrogels were fabricated, and their physical properties were characterized. ELMs were comprised of *E. coli* DH5α strain modified with an ampicillin-resistant plasmid. These bacteria were encapsulated within hydrogels made of 2-hydroxyethylacrylate (HEA) crosslinked with *N, N*'-methylenebisacrylamide (BIS) [24]. Cells within these ELMs (10HEA/0.1BIS) proliferated within the soft acrylic matrices and changed the global shape of the ELM (Fig.1b), due to the mechanical properties of the loaded bacteria [24,33]. Colony formation was observed during 72 h of incubation (Fig. 1c). To our knowledge, this is the first report to quantify the shape-changing behavior of composites of bacteria embedded within hydrogels.

It has been reported that encapsulation of microorganisms within acrylic hydrogels can result in a loss in the number of cells that are viable [34]. We performed experiments to study the viability of bacteria after being exposed to the selected monomer solutions (10HEA/0.1BIS, 15HEA/0.4BIS, and 20HEA/0.4BIS) for 2 min and 10 min (Fig. 2a). Cell viability was compared between control samples of cells exposed to LB-amp media and samples with cells that were exposed to the monomer solutions, without APS or TEMED. We note that cell viability was quantified after cells were exposed to the unpolymerized monomer solutions as cell viability at

large cell loadings within the hydrogel is difficult to quantify. The comparison between the cell viability of all the formulations with the control sample indicates that the toxicity of the monomer solutions increases as both monomer and crosslinker concentrations increase at both 2 min and 10 min exposure. Cell viability, as measured by counting the number of colony forming units per milliliter of solution of control samples, was significantly higher when comparing with the viability of all monomer solutions after the cells were exposed for 2 min (one-way ANOVA, $P < 0.0001$ for 10HEA/0.1BIS, 15HEA/0.4BIS, and 20HEA/0.4BIS) (Fig. 2a). After 10 min exposure, there was no significant difference between the cell viability of the 10HEA/0.1BIS formulation compared to the control (one-way ANOVA, $P > 0.05$), but viability was significantly higher in control samples compared to formulations 15HEA/0.4BIS and 20HEA/0.4BIS (one-way ANOVA, $P < 0.0001$ for both 15HEA/0.4BIS and 20HEA/0.4BIS) (Fig. 2a). Cell viability for the formulation 20HEA/0.4BIS compared to each of the other formulations was significantly lower at both 2 min (one-way ANOVA, $P < 0.0001$ for 20HEA/0.4BIS vs. 10HEA/0.1BIS and 15HEA/0.4BIS) and 10 min (one-way ANOVA, $P < 0.0001$ 20HEA/0.4BIS vs. 10HEA/0.1BIS and $P < 0.001$ 20HEA/0.4BIS vs. 15HEA/0.4BIS) (Fig. 2a). This latter result implies that exposing bacteria to very high monomer concentrations can critically decrease cell viability. For this reason, the 20HEA/0.4BIS was not used to make ELMs and was not further characterized in these studies. Future research in this area should focus on evaluating viable cells within polymerized ELMs to better understand the number of viable cells responsible for colony formation within ELMs.

Cell viability is also affected by the cell loading in the ELMs. In the synthesized composites, relatively large concentrations of cells are used. As the concentration of cells increases, the water content in the ELM precursor decreases. To understand the effect of the

effective increase in monomer concentration (in the solution), cell viability in formulations made with two lower cell loadings (medium and low), and a fixed monomer and crosslinker content (10HEA/0.1BIS, in the composite) was measured. These formulations were compared to formulations that were used to make ELMs with high cell loadings, discussed above, and to the respective LB-amp control samples. As expected, the number of colony forming units scaled with the loading of cells. The number of colony forming units per mL of precursor is significantly higher in high cell loading formulations compared to both low and medium cell loadings at both 2 min (one-way ANOVA, $P < 0.0001$ low vs. high and $P < 0.001$ medium vs. high) and 10 min of exposure (one-way ANOVA, $P < 0.0001$ low vs. high and $P < 0.001$ medium vs. high) (Fig. 2b, c). Between medium and low cell loadings, cell viability was significantly higher in medium cell loading formulations at both 2 min and 10 min of exposure (one-way ANOVA, $P < 0.0001$). For both low and medium cell loadings, there was no significant difference between their corresponding control at 2 min of exposure (unpaired *t*-tests, $P > 0.05$) (Fig. 2b, c). At 10 min of exposure, the cell viability of low cell loadings was significantly lower than its corresponding control and the cell viability of medium cell loadings was not significantly different as compared to its corresponding control (unpaired *t*-test, $P < 0.05$

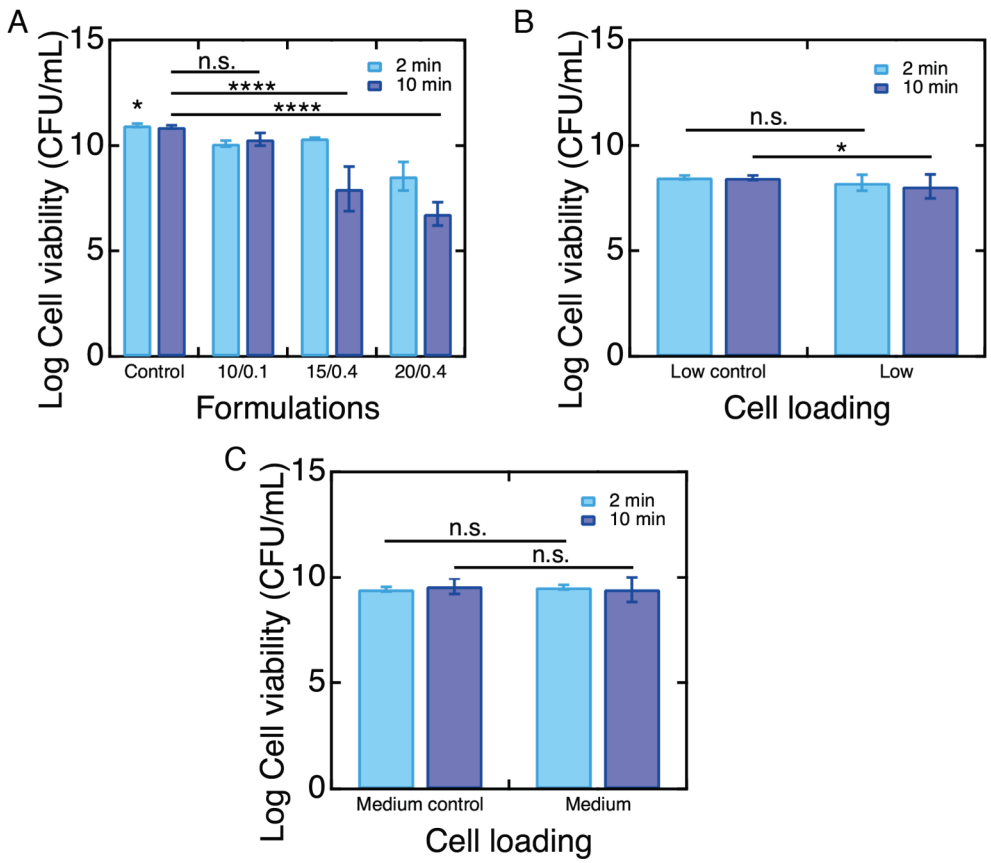

Figure 2: Cell viability of bacteria after exposure to pre-gel solutions
(A) Cell viability as a function of exposure to formulations with different monomer and crosslinker content. Control conditions represent exposure to LB media. (B) Cell viability as a function of time after exposure to the monomer solution with low cell loadings. (C) Cell viability as a function of time after exposure of the monomer solution with medium cell loadings. Bacteria was exposed to these pre-gel solutions for 2 min and 10 min. Monomer solutions are identified as the concentration (wt%) of HEA / concentration (wt%) of BIS. Statistical analysis: one-way ANOVA, *t*-test, * P-value < 0.05; **** P-value < 0.0001, not significant (n.s.). For (A) the (*) represents the statistical difference between the control and each of the formulations at 2 min incubation.

for low cell loadings and P > 0.05 for medium cell loadings) (Fig. 2b, c). These results indicate that the monomer solution does not substantially affect cell viability, when sufficient water is present. In contrast, as shown in Fig. 2a, when loading high cell concentrations, cell viability significantly decreased using the 10HEA/0.1BIS formulation as compared to the control at 2 min

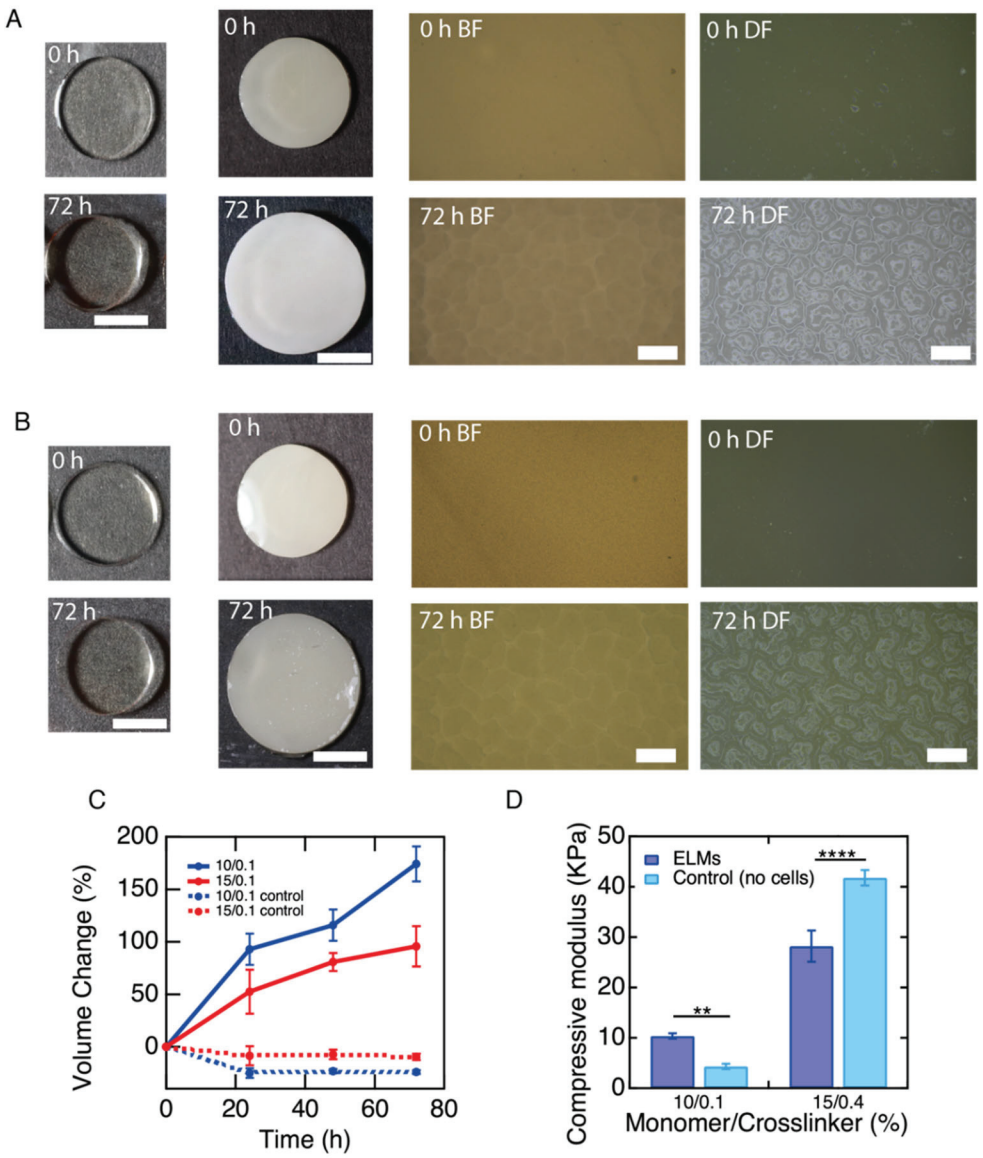

Figure 3: Volume change and mechanical properties of prokaryotic ELMs with different monomer and crosslinker contents and high cell loadings

(A) Macroscopic changes of control hydrogels made with 10HEA/0.1BIS (left) (Scale bar: 5 mm). Macroscopic changes of ELMs made with made with 10HEA/0.1BIS (center) (Scale bar: 5 mm). Microscopic changes of ELMs made with 10HEA/0.1BIS (right) (Scale bar: 200 μm). (B) Macroscopic changes of control hydrogels made with 15HEA/0.4BIS (left) (Scale bar: 5 mm). Macroscopic changes of ELMs made with made with 15HEA/0.4BIS (center) (Scale bar: 5 mm). Microscopic changes of ELMs made with 15HEA/0.4BIS (right) (Scale bar: 200 μm). (C) Volume changes of ELMs with varying monomer and crosslinker content as a function of time. (D) Compressive modulus as a function of monomer concentration. BF: bright field, DF: dark field Monomer solutions are identified as the concentration (wt%) of HEA / concentration (wt%) of BIS. Each data point represents the mean and error bars represent standard deviation. Trend lines are only intended to guide the eye. Statistical analysis: *t*-test, ** P-value < 0.01; **** P-value < 0.0001.

of exposure (one-way ANOVA, $P < 0.05$). It is likely that in this latter result, the decrease is

related to the high monomer solution: LB-amp ratio used to prepare the high cell density formulation, which causes the cells to be exposed to a more toxic environment derived from the presence of HEA and BIS.

The volume change of the ELMs can be tuned by controlling the stiffness of the ELM. As *E. coli* possesses a stiff cell envelope (Young's modulus = 50–150 MPa) [30], a key observation of this work is that the volume of the ELMs increases as these stiff cells proliferate within the compliant encapsulating matrix. Similar behavior was reported in our prior reports on yeast-containing ELMs [20,29] and a much earlier publication [30]. This proliferation-induced volume change can also be observed in bacteria-containing ELMs. The stiffness of the matrix is controlled by varying the HEA and BIS concentrations (10HEA/0.1BIS and 15HEA/0.4BIS). ELMs and control hydrogels without encapsulated cells were incubated in LB-amp media, which contains all necessary nutrients for bacterial growth, and incubated at 37 ºC for 72 h. After 72 h of incubation, macroscopic images show that control hydrogels for both formulations did not undergo volumetric expansions, while the ELMs are substantially larger (Fig. 3a, b). Optical micrographs show colonies formed and packed together within the ELMs (Fig. 3a, b). ELMs undergo volumetric changes that decrease from 174 % ± 16 % to 95% ± 45% as the encapsulating matrix increases in stiffness from 10 kPa ± 1 kPa to 28 kPa ± 3 kPa for 10HEA/0.1BIS and 15HEA/0.4BIS formulations, respectively (Fig. 3c, d). This behavior may be attributed to an increase in the elastic resistance from the matrix to the expanding bacterial colonies, which results in the decreased global expansion of the encapsulating matrix [20,29][30].

Compressive modulus of ELMs was further compared with the compressive modulus of hydrogels without encapsulated cells (control hydrogels). It was observed that ELMs made with

10HEA/0.1BIS were significantly stiffer as compared to control hydrogels made with the same formulation (4 kPa ± 1 kPa) (*t*-test, $P < 0.01$). However, ELMs made with 15HEA/0.4BIS were significantly more compliant than control hydrogel made with the same formulation (42 kPa ± 1 kPa) (*t*-test, $P < 0.0001$). These results suggest that there may be competing factors determining composite stiffness at these high cell loadings. For example, the presence of the stiff bacteria should reinforce the relatively compliant hydrogel matrix, but the polymerization reaction may also be affected by the cell loading.

Controlling the initial cell loading during ELM preparation can be used to further tune proliferation-driven volume changes. Low and medium cell loadings were used to make ELMs with constant monomer and crosslinker concentration (10HEA/0.1BIS). After incubating ELMs with medium and low cell loadings for 72 h, it was observed that the materials undergo macroscopic expansion and microscopic changes when compared with ungrown samples (Fig. 4a, b). We note that colony morphologies after growth differ in high, medium, and low cell loading ELMs. As shown in Figure 4b, colonies in low cell loading ELMs are apparently larger in volume as compared to medium and high cell loading ELMs. This behavior may be attributed to the larger spaces found between viable cells throughout the ELM matrix, which allows the colonies to occupy more space. In the high and medium cell loading ELMs, the colonies after growth are found to be more closely packed (Fig. 3a, 4a). Proliferation-driven volume changes of low cell loading ELMs after 72 h of growth were found to be lower (112 % ± 12 %) than the volume change of high cell loading ELMs (Fig. 4c). Although we note that the initial number of CFU loaded in the medium cell containing ELMs is 9× higher than the low cell

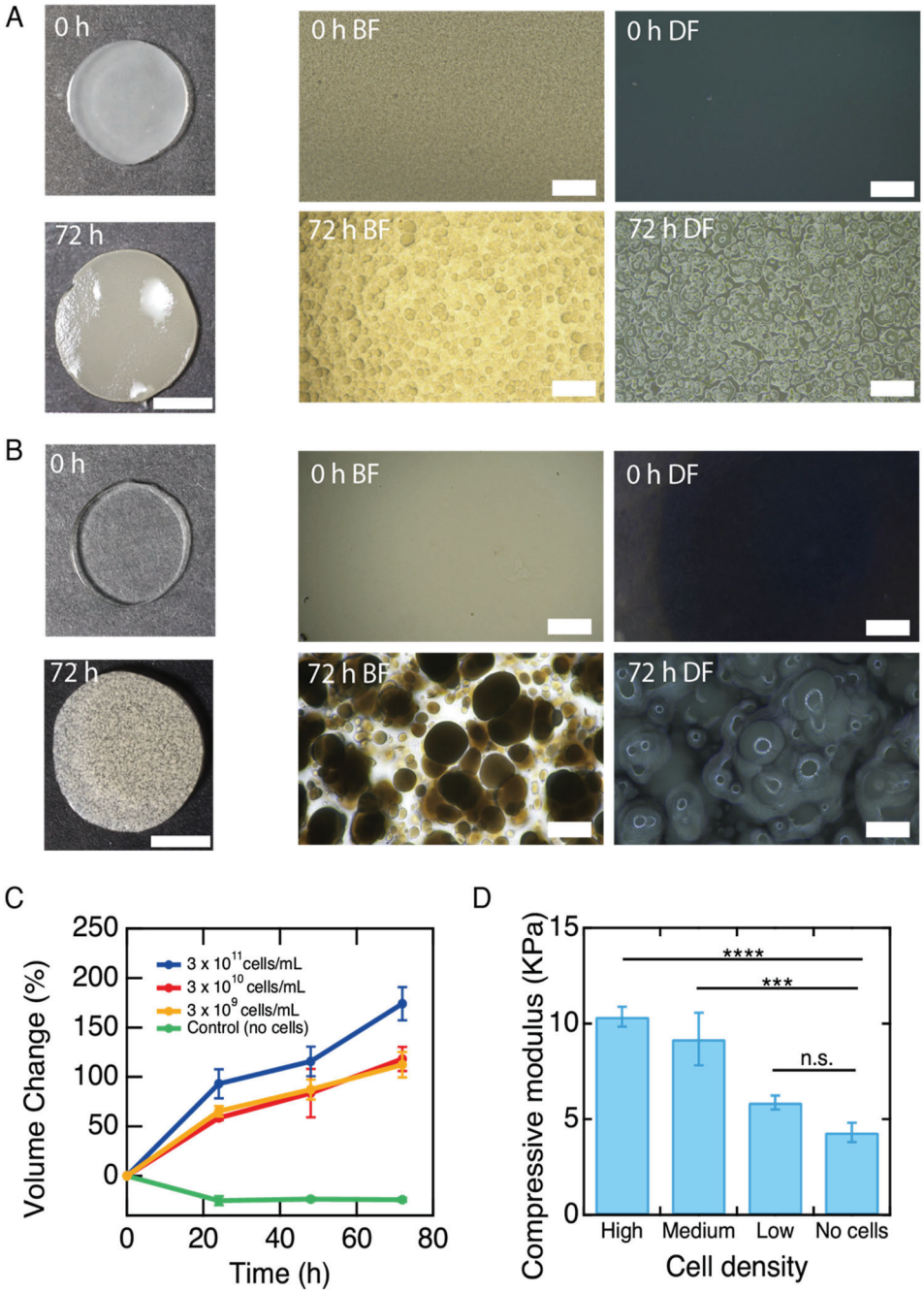

Figure 4: Volume change and mechanical properties of prokaryotic ELMs with different cell loadings and constant monomer and crosslinker content

(A) Macroscopic changes of ELMs made with medium cell loadings (left) (Scale bar: 5 mm). Microscopic changes of the same ELMs before and after 72 h of incubation (right) (Scale bar: 200 μm). (B) Macroscopic changes of ELMs made with low cell loadings (left) (Scale bar: 5 mm). Microscopic changes of the same ELMs before and after 72 h of incubation (right) (Scale bar: 200 μm). (C) Volume changes of ELMs with varying cell loadings as a function of time. (D) Compressive modulus as a function of cell density (BF: bright field, DF: dark field). The ELMs were comprised 10 wt% HEA and 0.1 wt% BIS. Each data point represents the mean and error bars represent standard deviation. Trend lines are only intended to guide the eye. Statistical analysis: one-way ANOVA, *** P-value < 0.001; **** P-value < 0.0001; not significant (n.s.).

containing ELM, the volume changes throughout the incubation period for both materials are very similar. This similarity may be attributed to the larger colonies that formed within the low cell loading ELMs. These results show that bacterial proliferation changes the global shape of the ELMs, and these changes can be controlled, although not in a linear fashion, by modulating the initial cell loading within synthetic matrices. These nonlinear relationships between volume change and cell loading are likely modulated by a variety of competing factors. For example, the presence of bacteria may alter the polymerization reaction leading to difference in the elastic modulus of the matrix [29]. Furthermore, larger cell loadings may also reduce the availability of nutrients within the material.

As the mechanical properties of ELMs can control the proliferation-induced volume changes, we compared Young's modulus between ELMs with different cell loadings and control hydrogels made with 10HEA/0.1BIS. After measuring compressive modulus, the results indicate that there is no significant difference between the compressive modulus of ELMs made with low cell loading (6 kPa $\pm$ 1 kPa) and the compressive modulus of control hydrogels (4 kPa $\pm$ 1 kPa) (one-way ANOVA, $P > 0.05$). However, the compressive moduli of medium cell loading ELMs (9 kPa $\pm$ 1 kPa) and high cell loading ELMs (10 kPa $\pm$ 1 kPa) were significantly higher as compared to the control hydrogels (one-way ANOVA, $P < 0.001$ for medium vs. control and $P < 0.0001$ for high vs. control) (Fig. 4d). These mechanical studies suggest that the presence of stiff bacteria within hydrogels increases the stiffness of the ELM composite of this composition.

3.2 Bacterial delivery from ELMs

Control over the mechanical properties and the initial cell loading of ELMs are important factors to adjust the number of cells delivered to the surrounding media during cell proliferation. We quantified the number of cells present in the media (CFU/mL of media) surrounding ELMs

with varying stiffnesses and with low, medium, and high cell loadings. ELMs were grown in LB-amp media for a total of 26 h, where aliquots (100 μL) of the growth media were collected at 2 h, 4 h, and 24 h incubation + 2 h. It is important to note that after 24 h of incubation, ELMs were washed in LB-amp and then placed in fresh LB-amp to collect aliquots of the media after an additional 2 h incubation. We quantified the number of cells present through the 26 h of incubation (Fig. 5 and Fig. 6). We note that our measurement of delivered viable cells is imperfect as viable cells that are released can continue to proliferate. We could not devise a method to overcome this issue, but the number of cells in the media should still be proportional to the number of cells released from the gel.

For ELMs with varying stiffness, cell delivery from lower elastic modulus formulation 10HEA/0.1BIS was significantly higher as compared to 15HEA/0.4BIS (*t*-test, unpaired, P < 0.0001) for the first 2 h of incubation (Fig. 5a). The low cell delivery in 15HEA/0.4BIS

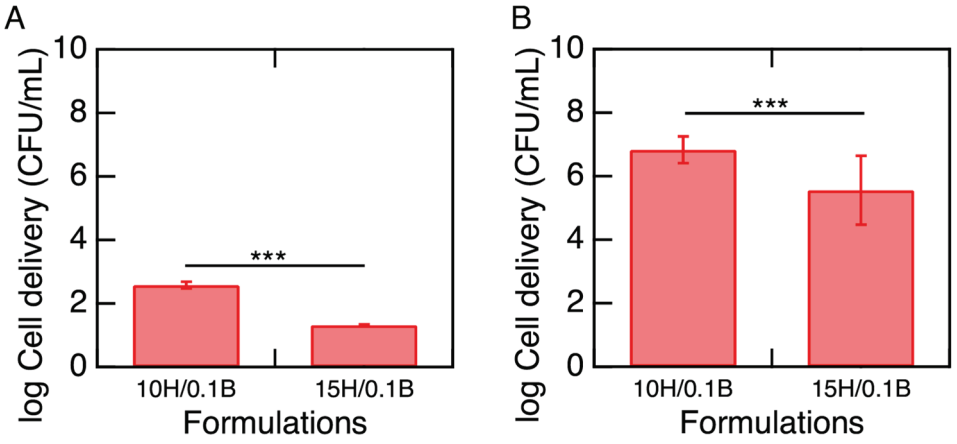

Figure 5: Cell delivery as a function of ELMs with varying crosslinking density
(A) Cell delivery as measured by the number of cells in the media surrounding the ELM as a function of ELM formulations after the initial 2 h of incubation. (B) Log cell delivery as measured by the number of cells in the media surrounding the ELM as a function of ELM formulation after incubation for 24 h + 2 h. Monomer solutions are identified as the concentration (wt%) of HEA / concentration (wt%) of BIS. Each data point represents the mean and error bars represent standard deviation. Statistical analysis: *t*-test, *** P-value < 0.001.

formulations may be attributed to their high Young's modulus, where it was observed that the encapsulated cells find it challenging to proliferate within stiff matrices, and therefore, to be released from the matrix.

After 24 h of incubation, the growth media was replaced, and the cell delivery was measured in the next 2 h of incubation. This cell delivery was observed to be significantly higher in both formulations as compared to the delivery at the first 2 h of incubation (*t*-test, paired, $P < 0.0001$) (Fig. 6b). At this incubation time point, cells are delivered in a substantially higher quantity. Likely additional delivery is due to the larger number of cells in the composite that formed during the first 24 h of incubation. Between 10HEA/0.1BIS and15HEA/0.4BIS, there was a significantly higher cell delivery from 10HEA/0.1BIS ELMs, also thought to be due to the difference in material stiffness (*t*-test, unpaired, $P < 0.001$).

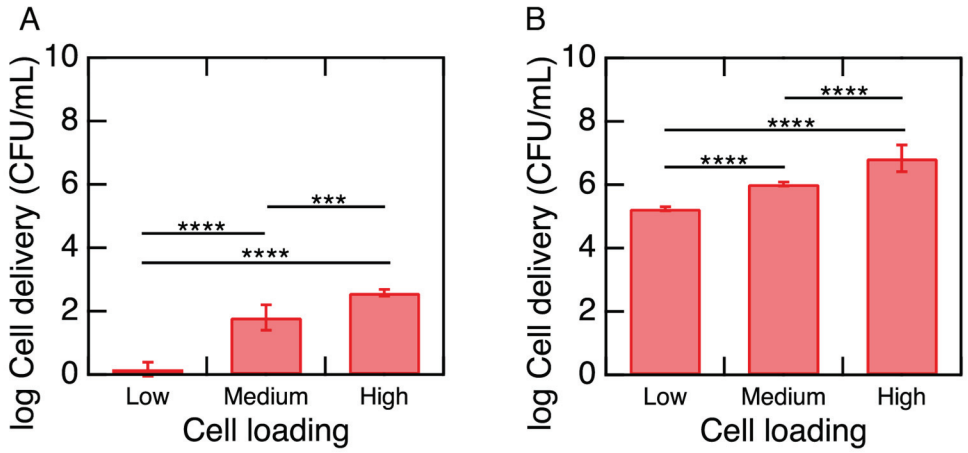

Figure 6: Cell delivery as a function cell loading
(A) Cell delivery as measured by the number of cells in the media surrounding the ELM after 2 h of incubation(B) Cell delivery as measured by the number of cells in the media surrounding the ELM after incubation for 24 h + 2 h. The ELMs were comprised 10 wt% HEA and 0.1 wt% BIS. Each data point represents the mean and error bars represent standard deviation. Statistical analysis: one-way ANOVA, *** P-value < 0.001; **** P-value < 0.0001.

The initial cell loading within ELMs also affects the number of delivered cells. We compared the cell delivery of ELMs after 2 h of incubation and observed that cell delivery at low

cell loadings was significantly lower as compared to both medium and high cell loadings (one-way ANOVA, $P < 0.0001$). Comparing medium and high cell loadings, cell delivery was significantly lower in the medium cell loading ELMs (one-way ANOVA, $P < 0.001$). The same relative behavior was observed at 24 h + 2 h of incubation for all cell loadings (one-way ANOVA, $P < 0.0001$ for all comparisons). For all cell loadings, cell delivery was higher at 24 h + 2 h as compared to their initial 2 h (one-way ANOVA, $P < 0.0001$). This information tells us that, over these ranges of loaded cell densities, we can obtain control over the cells delivered to the surrounding media. Using the results described thus far, we selected the formulation 10HEA/0.1BIS with high cell loading for further cell delivery studies.

The cell delivery from the cut ELM discs was also compared with the molded ELM discs of the same dimensions. Comparing cell delivery after 2 h, 24 h + 2 h, and 48 h + 2 h, it was observed that uncut ELMs had lower cell delivery at 2 h compared to the cut ELMs, but no significant difference existed after 24 h + 2 h and 48 h + 2 h (*t*-test, unpaired, $P > 0.05$) (Fig. S1). The lack of substantial differences suggests that cutting the sample is not critical for cell release.

To better quantify the number of released cells as compared to cells that proliferated in the media, we measured the number of CFU in growth media under two conditions. In condition 1, the ELM was placed in fresh media for 30 mins and then removed. CFUs were counted immediately and again 90 mins later. In condition two, the ELM remained in the media for the entire two hours, and CFUs were counted at both 30 mins and 2 hours. When the ELMs were removed from the growth media after 30 min of incubation (Condition 1), no significant difference was observed between the number of cells in the media at 30 min and 2 h (*t*-test, unpaired, $P > 0.05$) (Fig. S2a). However, when the ELMs were present in the growth media for the entire 2 h of incubation (Condition 2), a significantly higher number of cells were present in

the media at 2 h compared to 30 min (*t*-test, unpaired, $P < 0.01$) (Fig. S2b). These results suggest that cell release, and not proliferation of released cells, is primarily responsible for the numbers of observed CFU.

3.3 Probiotic ELMs delivery and co-culture with a pathogen

ELMs provide a promising approach for *in situ* delivery of probiotics. The design of ELMs capable of delivering probiotics continuously could ultimately be harnessed to create devices to locally deliver cells that act against pathogen fitness. For example, some *E. coli* strains can cause asymptomatic bacteriuria and other strains induce symptomatic urinary tract infections (UTI) [35,36]. An asymptomatic bacteriuric (ABU) *E. coli* strain, ABU 83972, has been identified as a potentially safe and effective probiotic for therapeutic and prophylactic strategies to prevent UTIs [37]. ABU 83972 has been shown to outcompete the growth of uropathogenic *E. coli* (UPEC) strains such as CFT073. ABU 83972 strain exhibits a higher growth rate and doubling time compared to many UPEC strains including CFT073 [37,38]. Furthermore, the genome of ABU 83972 strain is not known to encode potential antibacterial molecules that could allow this strain to kill or inhibit UPEC growth [39]. Hence, the competition for nutrients is the likely explanation for the ability of ABU 83972 to outcompete UPECs such as CFT073. Nevertheless, ABU 83972 is not capable of persisting in the bladder in patients that void normally as it does not adhere to the bladder walls. A strategy that uses the ELM delivery mechanism described in this research could be potentially utilized in the development of devices to treat UTIs [35].

We fabricated ELMs encapsulating high cell loadings of ABU 83972 and studied their volume changes, cell delivery behavior, and the ability to compete with a UPEC strain *in vitro*.

Following the procedure to encapsulate DH5α, we synthesized ELMs encapsulating high ABU

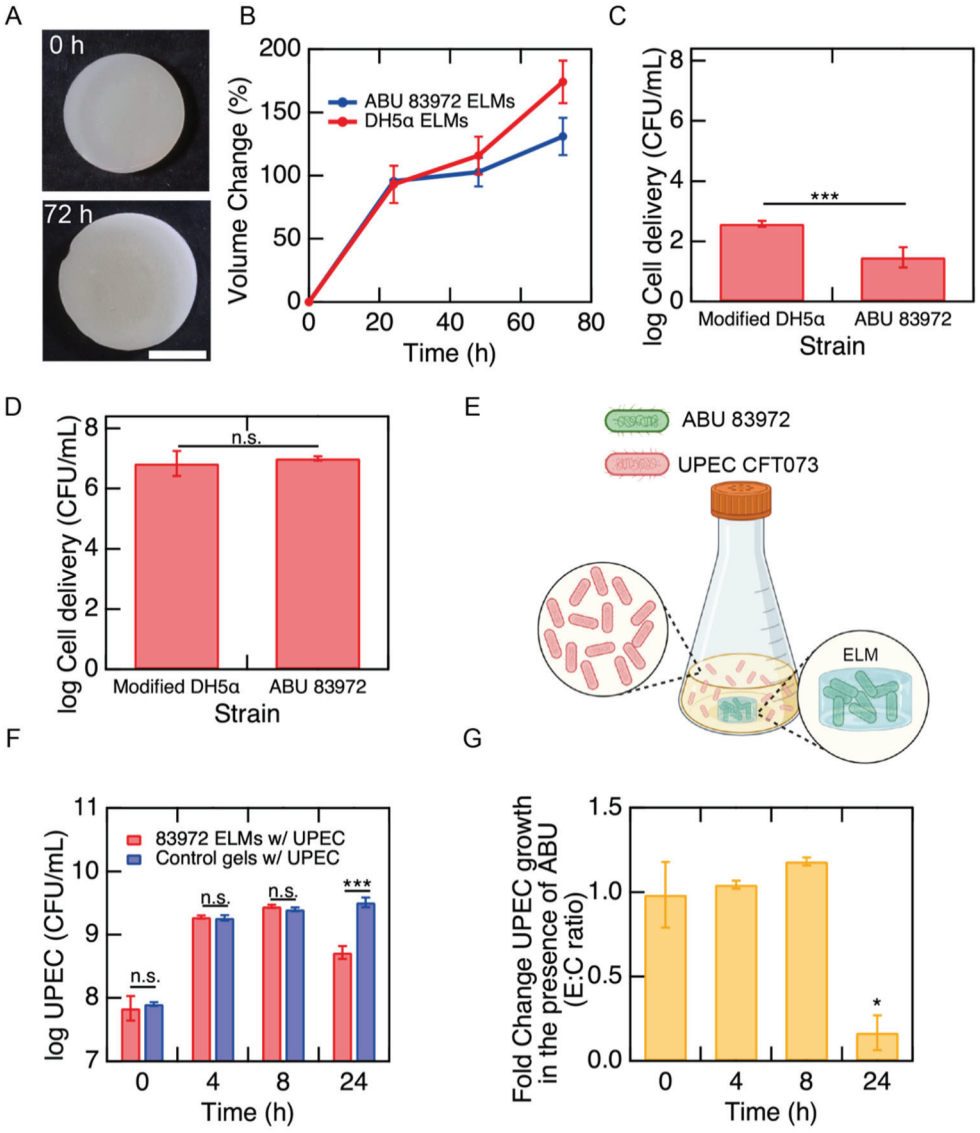

Figure 7: Probiotic ELMs can be used to compete with uropathogenic strains
(A) Macroscopic expansion of an ABU 83972 ELM before and after incubation for 72 h (Scale bar: 5 mm). (B) Volume change as a function of time of ABU 83972 ELMs and high cell loading ELMs made with 10HEA/0.1BIS. (C) Cell delivery as measured by the number of cells in the media surrounding the ELMs containing *E. coli* strains DH5α and ABU 83972 after 2 h of incubation and after (D) 24 h + 2 h of incubation. (E) Schematic of the ABU 83972 ELM and free floating CFT073 co-culture. (F) Cell growth of UPEC strain as a function of time for UPEC in the presence of ABU 83972 ELMs and control hydrogels. (G) Fold change in the growth of UPEC with control samples to the growth of UPEC in the presence of ABU 83972 (E:C, Experimental:Control). Each data point represents the mean and error bars represent standard deviation. Trend lines are only intended to guide the eye. Statistical analysis: *t*-test, one-way ANOVA, * P-value < 0.05; *** P-value < 0.001. For (G) the (*) represents the statistical difference between the fold change at 24 h as compared to 0, 4, 8 h.

cell loadings. These probiotic ELMs can undergo volumetric expansions of 130 % ± 15 % (Fig. 7a, b) after 72 h of incubation. Comparing cell delivery after 2 h and 24 h + 2 h with the delivery of DH5α ELMs, it was observed that ABU 83972 ELMs had a significantly lower cell delivery at 2 h but that no significant difference existed at 24 h + 2 h (unpaired *t*-tests, $P < 0.001$ for 2 h, $P > 0.05$ for 24 h + 2 h) (Fig. 7c, d).

We conducted direct co-culture experiments at a 1:1 ratio of CFU/mL present in the probiotic ELMs and the CFU/mL of the free-floating UPEC strain, CFT073, resistant to the antibiotic kanamycin (Fig. 7e). We focused on quantifying UPEC growth after co-cultures were incubated for 0 h, 4 h, 8 h, and 24 h. This growth behavior was compared against co-cultures of UPEC with control hydrogels which do not contain any ABU. As shown in Figure 7f, we observed that the growth of the UPEC strain co-cultured with ABU was not significantly different as compared to the UPEC growth in the presence of control hydrogels during the first 8 h of incubation (*t*-test, unpaired, $P > 0.05$). After 24 h of incubation, UPEC growth was significantly higher without the presence of ABU (*t*-test, unpaired, $P < 0.001$) (Fig. 7f). This is also reflected in a decreased fold change in the UPEC growth incubated with ABU compared to UPEC co-cultures with control gels (Fig. 7g). We envision that a multifunctional materials platform could be designed for biomedical applications by coupling shape change and prokaryotic delivery. This platform could enable the release of encapsulated therapeutics from a reservoir in addition to the controlled delivery of probiotics to specific places in the body [20].

3.4 Conclusions

ELMs comprised of bacteria encapsulated in a synthetic acrylic matrix release cells and undergo an increase in volume driven by embedded cell proliferation. By increasing the stiffness

of ELMs, we observed that the composites undergo less volume change and that the delivered number of cells is significantly lowered. ELMs that begin with a lower concentration of embedded cells also release few cells during culture. ELMs could potentially be used in multifunctional biomedical devices where the controlled delivery of bacteria probiotics enables therapeutic action. For example, we envision future devices where shape change triggers delivery of a therapeutic while the probiotic delivery occurs resulting in multimodal, localized approaches to treating infections, such as UTI.

4. Acknowledgements

Research reported in this publication was partially supported by the National Institute Of Biomedical Imaging And Bioengineering of the National Institutes of Health under Award Number R56EB032395 (T.H.W., S.S., and P.E.Z). This material is also partially based upon work supported by the National Science Foundation under Grant No. 2039425 (T.H.W), and National Institutes of Health under Grant Nos. DK114224 (S.S).The Funders had no role in study design, data collection and analysis, decision to publish, or preparation of the manuscript. The content is solely the responsibility of the authors and does not necessarily represent the official views of the funders. We thank Panatda Saenkham-Huntsinger for technical assistance and helpful discussions on competition experiments. We thank Zachary Campbell and Patrick Smith for providing *E.coli* DH5α (transformed with pAAV-Syn-GFP plasmid). Graphics were created with BioRender.com.

5. Declaration of competing interest

The authors declare no competing interests.

6. References

[1] P.Q. Nguyen, N.-M.D. Courchesne, A. Duraj-Thatte, P. Praveschotinunt, N.S. Joshi, Engineered Living Materials: Prospects and Challenges for Using Biological Systems to Direct the Assembly of Smart Materials, Adv Mater. 30 (2018) 1704847. https://doi.org/10.1002/adma.201704847.

[2] C. Gilbert, T. Ellis, Biological Engineered Living Materials - growing functional materials with genetically-programmable properties., Acs Synth Biol. 8 (2018) 1–15. https://doi.org/10.1021/acssynbio.8b00423.

[3] L.K. Rivera-Tarazona, Z.T. Campbell, T.H. Ware, Stimuli-responsive engineered living materials, Soft Matter. 17 (2021) 785–809. https://doi.org/10.1039/d0sm01905d.

[4] A. Rodrigo-Navarro, S. Sankaran, M.J. Dalby, A. del Campo, M. Salmeron-Sanchez, Engineered living biomaterials, Nat Rev Mater. 6 (2021) 1175–1190. https://doi.org/10.1038/s41578-021-00350-8.

[5] A.D. Lantada, J.G. Korvink, M. Islam, Taxonomy for engineered living materials, Cell Reports Phys Sci. 3 (2022) 100807. https://doi.org/10.1016/j.xcrp.2022.100807.

[6] C. Gilbert, T.-C. Tang, W. Ott, B.A. Dorr, W.M. Shaw, G.L. Sun, T.K. Lu, T. Ellis, Living materials with programmable functionalities grown from engineered microbial co-cultures, Nat Mater. 20 (2021) 691–700. https://doi.org/10.1038/s41563-020-00857-5.

[7] X. Liu, Y. Yang, M.E. Inda, S. Lin, J. Wu, Y. Kim, X. Chen, D. Ma, T.K. Lu, X. Zhao, Magnetic Living Hydrogels for Intestinal Localization, Retention, and Diagnosis, Adv Funct Mater. (2021) 2010918. https://doi.org/10.1002/adfm.202010918.

[8] L. Xu, X. Wang, F. Sun, Y. Cao, C. Zhong, W.-B. Zhang, Harnessing proteins for engineered living materials, Curr Opin Solid State Mater Sci. 25 (2021) 100896. https://doi.org/10.1016/j.cossms.2020.100896.

[9] M. Mimee, P. Nadeau, A. Hayward, S. Carim, S. Flanagan, L. Jerger, J. Collins, S. McDonnell, R. Swartwout, R.J. Citorik, V. Bulović, R. Langer, G. Traverso, A.P. Chandrakasan, T.K. Lu, An ingestible bacterial-electronic system to monitor gastrointestinal health, Science. 360 (2018) 915–918. https://doi.org/10.1126/science.aas9315.

[10] S. Guo, E. Dubuc, Y. Rave, M. Verhagen, S.A.E. Twisk, T. van der Hek, G.J.M. Oerlemans, M.C.M. van den Oetelaar, L.S. van Hazendonk, M. Brüls, B.V. Eijkens, P.L. Joostens, S.R. Keij, W. Xing, M. Nijs, J. Stalpers, M. Sharma, M. Gerth, R.J.E.A. Boonen, K. Verduin, M. Merkx, I.K. Voets, T.F.A. de Greef, Engineered Living Materials Based on Adhesin-Mediated Trapping of Programmable Cells., Acs Synth Biol. 9 (2020) 475–485. https://doi.org/10.1021/acssynbio.9b00404.

[11] S. Han, E.K. Choi, W. Park, C. Yi, N. Chung, Effectiveness of expanded clay as a bacteria carrier for self-healing concrete, Appl Biol Chem. 62 (2019) 19. https://doi.org/10.1186/s13765-019-0426-4.

[12] L.K. Rivera-Tarazona, T. Shukla, K.A. Singh, A.K. Gaharwar, Z.T. Campbell, T.H. Ware, 4D Printing of Engineered Living Materials, Adv Funct Mater. (2021) 2106843. https://doi.org/10.1002/adfm.202106843.

[13] J.J. Hay, A. Rodrigo-Navarro, M. Petaroudi, A.V. Bryksin, A.J. García, T.H. Barker, M.J. Dalby, M. Salmeron-Sanchez, Bacteria-Based Materials for Stem Cell Engineering, Adv Mater. 30 (2018) 1804310. https://doi.org/10.1002/adma.201804310.

[14] P. Praveschotinunt, A.M. Duraj-Thatte, I. Gelfat, F. Bahl, D.B. Chou, N.S. Joshi, Engineered E. coli Nissle 1917 for the delivery of matrix-tethered therapeutic domains to the gut, Nat Commun. 10 (2019) 5580. https://doi.org/10.1038/s41467-019-13336-6.

[15] T.G. Johnston, S.-F. Yuan, J.M. Wagner, X. Yi, A. Saha, P. Smith, A. Nelson, H.S. Alper, Compartmentalized microbes and co-cultures in hydrogels for on-demand bioproduction and preservation, Nat Commun. 11 (2020) 563. https://doi.org/10.1038/s41467-020-14371-4.

[16] H.W. Kua, S. Gupta, A.N. Aday, W.V. Srubar, Biochar-immobilized bacteria and superabsorbent polymers enable self-healing of fiber-reinforced concrete after multiple damage cycles, Cem Concr Compos. 100 (2019) 35–52. https://doi.org/10.1016/j.cemconcomp.2019.03.017.

[17] A.W. Feinberg, A. Feigel, S.S. Shevkoplyas, S. Sheehy, G.M. Whitesides, K.K. Parker, Muscular Thin Films for Building Actuators and Powering Devices, Science. 317 (2007) 1366–1370. https://doi.org/10.1126/science.1146885.

[18] L.K. Rivera-Tarazona, V.D. Bhat, H. Kim, Z.T. Campbell, T.H. Ware, Shape-morphing living composites, Sci Adv. 6 (2020) eaax8582. https://doi.org/10.1126/sciadv.aax8582.

[19] A.E. Smith, Z. Zhang, C.R. Thomas, K.E. Moxham, A.P.J. Middelberg, The mechanical properties of Saccharomyces cerevisiae, Proc National Acad Sci. 97 (2000) 9871–9874. https://doi.org/10.1073/pnas.97.18.9871.

[20] L.K. Rivera-Tarazona, T. Shukla, K.A. Singh, A.K. Gaharwar, Z.T. Campbell, T.H. Ware, 4D Printing of Engineered Living Materials, Adv Funct Mater. 32 (2022) 2106843. https://doi.org/10.1002/adfm.202106843.

[21] D. Czerucka, T. Piche, P. Rampal, Review article: yeast as probiotics -- Saccharomyces boulardii., Aliment Pharm Therap. 26 (2007) 767–78. https://doi.org/10.1111/j.1365-2036.2007.03442.x.

[22] J.R. Bober, C.L. Beisel, N.U. Nair, Synthetic Biology Approaches to Engineer Probiotics and Members of the Human Microbiota for Biomedical Applications, Annu Rev Biomed Eng. 20 (2018) 1–24. https://doi.org/10.1146/annurev-bioeng-062117-121019.

[23] T.-C. Tang, B. An, Y. Huang, S. Vasikaran, Y. Wang, X. Jiang, T.K. Lu, C. Zhong, Materials design by synthetic biology, Nat Rev Mater. 6 (2020) 332–350. https://doi.org/10.1038/s41578-020-00265-w.

[24] H.H. Tuson, G.K. Auer, L.D. Renner, M. Hasebe, C. Tropini, M. Salick, W.C. Crone, A. Gopinathan, K.C. Huang, D.B. Weibel, Measuring the stiffness of bacterial cells from growth rates in hydrogels of tunable elasticity, Mol Microbiol. 84 (2012) 874–891. https://doi.org/10.1111/j.1365-2958.2012.08063.x.

[25] B. Pabst, B. Pitts, E. Lauchnor, P.S. Stewart, Gel-Entrapped Staphylococcus aureus Bacteria as Models of Biofilm Infection Exhibit Growth in Dense Aggregates, Oxygen Limitation, Antibiotic Tolerance, and Heterogeneous Gene Expression., Antimicrob Agents Ch. 60 (2016) 6294–301. https://doi.org/10.1128/aac.01336-16.

[26] S. Bhusari, S. Sankaran, A. del Campo, Regulating Bacterial Behavior within Hydrogels of Tunable Viscoelasticity, Adv Sci. (2022) e2106026. https://doi.org/10.1002/advs.202106026.

[27] T.-C. Tang, E. Tham, X. Liu, K. Yehl, A.J. Rovner, H. Yuk, C. de la Fuente-Nunez, F.J. Isaacs, X. Zhao, T.K. Lu, Hydrogel-based biocontainment of bacteria for continuous sensing and computation, Nat Chem Biol. (2021) 1–8. https://doi.org/10.1038/s41589-021-00779-6.

[28] W. Xu, P.M.M. Nouri, S. Demoustier-Champagne, K. Glinel, A.M. Jonas, Encapsulation of Commensal Skin Bacteria within Membrane-in-Gel Patches, Adv Mater Interfaces. (2022) 2102261. https://doi.org/10.1002/admi.202102261.

[29] L.K. Rivera-Tarazona, V.D. Bhat, H. Kim, Z.T. Campbell, T.H. Ware, Shape-morphing living composites, Sci Adv. 6 (2020) eaax8582. https://doi.org/10.1126/sciadv.aax8582.

[30] H.H. Tuson, G.K. Auer, L.D. Renner, M. Hasebe, C. Tropini, M. Salick, W.C. Crone, A. Gopinathan, K.C. Huang, D.B. Weibel, Measuring the stiffness of bacterial cells from growth rates in hydrogels of tunable elasticity, Mol Microbiol. 84 (2012) 874–891. https://doi.org/10.1111/j.1365-2958.2012.08063.x.

[31] T.-C. Tang, B. An, Y. Huang, S. Vasikaran, Y. Wang, X. Jiang, T.K. Lu, C. Zhong, Materials design by synthetic biology, Nat Rev Mater. 6 (2020) 332–350. https://doi.org/10.1038/s41578-020-00265-w.

[32] J.R. Bober, C.L. Beisel, N.U. Nair, Synthetic Biology Approaches to Engineer Probiotics and Members of the Human Microbiota for Biomedical Applications, Annu Rev Biomed Eng. 20 (2018) 1–24. https://doi.org/10.1146/annurev-bioeng-062117-121019.

[33] S. Bhusari, S. Sankaran, A. del Campo, Regulating Bacterial Behavior within Hydrogels of Tunable Viscoelasticity, Adv Sci. 9 (2022) 2106026. https://doi.org/10.1002/advs.202106026.

[34] H.N. Burrill, L.E. Bell, P.F. Greenfield, D.D. Do, Analysis of Distributed Growth of Saccharomyces cerevisiae Cells Immobilized in Polyacrylamide Gel., Appl Environ Microb. 46 (1983) 716–21. https://doi.org/10.1128/aem.46.3.716-721.1983.

[35] F. Sundén, L. Håkansson, E. Ljunggren, B. Wullt, Escherichia coli 83972 Bacteriuria Protects Against Recurrent Lower Urinary Tract Infections in Patients With Incomplete Bladder Emptying, J Urology. 184 (2010) 179–185. https://doi.org/10.1016/j.juro.2010.03.024.

[36] B. Wullt, C. Svanborg, Deliberate Establishment of Asymptomatic Bacteriuria—A Novel Strategy to Prevent Recurrent UTI, Pathogens. 5 (2016) 52. https://doi.org/10.3390/pathogens5030052.

[37] V. Roos, G.C. Ulett, M.A. Schembri, P. Klemm, The Asymptomatic Bacteriuria Escherichia coli Strain 83972 Outcompetes Uropathogenic E. coli Strains in Human Urine, Infect Immun. 74 (2006) 615–624. https://doi.org/10.1128/iai.74.1.615-624.2006.

[38] V.S. Forsyth, C.E. Armbruster, S.N. Smith, A. Pirani, A.C. Springman, M.S. Walters, G.R. Nielubowicz, S.D. Himpsl, E.S. Snitkin, H.L.T. Mobley, Rapid Growth of Uropathogenic Escherichia coli during Human Urinary Tract Infection, Mbio. 9 (2018) e00186-18. https://doi.org/10.1128/mbio.00186-18.

[39] R.M. Vejborg, C. Friis, V. Hancock, M.A. Schembri, P. Klemm, A virulent parent with probiotic progeny: comparative genomics of Escherichia coli strains CFT073, Nissle 1917 and ABU 83972, Mol Genet Genomics. 283 (2010) 469–484. https://doi.org/10.1007/s00438-010-0532-9.